Journal of the Physical Society of Japan
Vol. 74, No. 2, February, 2005, pp. 511–514

Photo-induced Insulator–Metal Transition in an Organic Conductor α-(BEDT-TTF)$_2$I$_3$

Naoya TAJIMA*, Jun-ichi FUJISAWA, Nobuko NAKA†, Teruya ISHIHARA, Reizo KATO, Yutaka NISHIO[1] and Koji KAJITA[1]

RIKEN, 2-1 Hirosawa, Wako, Saitama, 351-0198
[1]*Department of Physics, Toho University, 2-2-1 Miyama, Funabashi, Chiba 274-8510*

(Received August 28, 2004)

Photo-switching between a charge-ordered insulating (CO) state and a metallic (M) state has been successfully realized in an organic conductor α-(BEDT-TTF)$_2$I$_3$ at low temperatures. The large photocurrent induced by the pulsed laser excitation with a photon energy of 2.6 eV had two components. The fast-decaying component had a life time of 120 ns. The subsequent one rose slowly (after about 0.7 μs) and remained as long as an electric field above 470 V/cm was applied. The dependences of these two components on laser power, applied voltage, and the onset of pulsed voltage were examined. It has been clearly demonstrated that the second component has prominent thresholds for both laser power and voltage. For each component, the resistivity decreased by about seven orders of magnitude from about 4 MΩ·cm to less than 0.4 Ω·cm at 4 K.

KEYWORDS: α-(BEDT-TTF)$_2$I$_3$, charge-ordered insulating state, photoconductivity
DOI: 10.1143/JPSJ.74.511

For many years, organic conductors have been fascinated physicists as basic materials for searching new physics. A rich variety of materials is one of the characteristics of organic conductors. Recently, the electronic states of organic conductors have been revealed to be controlled by pressure,[1–4] electric field[5,6] and magnetic field,[7–9] effectively. We report here a photo-induced insulator–metal transition in an organic conductor α-(BEDT-TTF)$_2$I$_3$ at low temperatures.

The organic conductor α-(BEDT-TTF)$_2$I$_3$ is a member of the (BEDT-TTF)$_2$I$_3$ family.[10] All the crystals in this family consist of an alternate arrangement of a conductive layer of BEDT-TTF molecules and an insulating layer of I_3^- anions as shown in the inset of Fig. 1.[10–13] The difference among them lies in the arrangement and orientation of BEDT-TTF molecules within the conducting plane and this difference gives rise to variations in the transport phenomena. Most of the members of this family are two-dimensional metals with large Fermi surfaces and some of them are superconducting with T_c values of several Kelvin.[11–13] On the other hand, α-(BEDT-TTF)$_2$I$_3$ exhibits exceptional characteristics. At ambient pressure, this salt is metallic down to 135 K, where it undergoes a phase transition to an insulator as shown in Fig. 1.[10] According to the theoretical investigation by Kino and Fukuyama[14] and the experimental work by Takano *et al.*,[15] this transition is due to the charge-ordering. This implies that electron correlation plays an important role in the transport phenomena of this material.

The above phase transition is suppressed by the application of hydrostatic pressure. The system under a high hydrostatic pressure appears to be a metal over the whole temperature region. The transport property of carriers in this metallic state, however, is quite unique and we reported a new type of transport phenomenon in this system.[3] The conductivity is almost constant between 300 and 1.5 K. In the same temperature region, however, both the carrier (hole) density and mobility change by about six orders of magnitude. At low temperatures, the carrier system is in a state with a high mobility [3×10^5 cm^2/(V·s)] and a low density (5×10^{15} cm^{-3}). Notably, these changes in carrier mobility and density over many orders of magnitude occur in a way so that they cancel each other out, which results in the temperature-independent conductivity.[3] We have no other examples of such conductors among both organic and inorganic materials. In this respect, we claim that α-(BEDT-TTF)$_2$I$_3$ under high pressures is a new type of conductor. The mechanism of this phenomenon, however, remains to be clarified and extended experimental surveys are necessary.

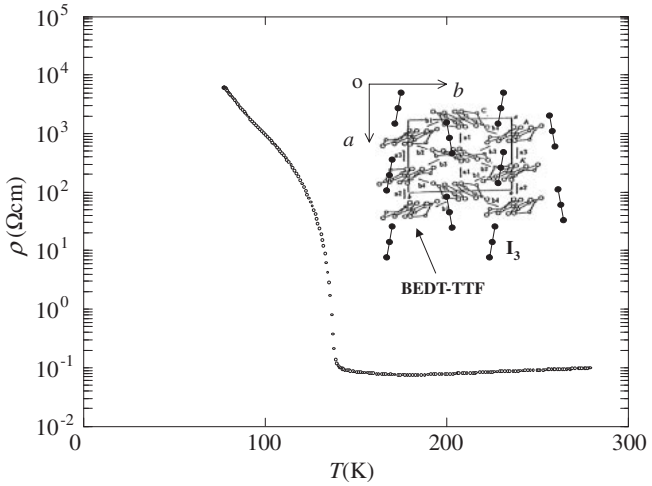

Fig. 1. Temperature dependence of resistivity for α-(BEDT-TTF)$_2$I$_3$ at ambient pressure. The inset shows the crystal structure viewed from the c^*-axis.

In this study, we irradiated light on the crystal of α-(BEDT-TTF)$_2$I$_3$ and examined the behavior of photo-created carriers in the charge-ordered insulating state at low temperatures. We have demonstrated that α-(BEDT-TTF)$_2$I$_3$ exhibits photo switching between the charge-ordered insu-

*E-mail: taji@riken.jp
†Present address: Department of Applied Physics, The University of Tokyo, 7-3-1 Hongo, Bunkyo-ku, Tokyo 113-8656.

lating (CO) state and the metallic (M) state at low temperatures and high-excitation-intensity conditions. In particular, the discovery of a durable photocurrent under a high electric field should be emphasized. Similar behaviors were reported for the CO state of perovskite manganite $Pr_{0.7}Ca_{0.3}MnO_3$ by Miyano *et al.*[16,17] And, there are some reports on the photo-induced insulator-to-metal transition in organic conductors.[18,19] To our knowledge, however, this is the first report of the photo-induced persistently conducting state in organic conductors.

Single crystals prepared by the electrolysis method were parallelepiped with typical dimensions of $0.8 \times 0.5 \times 0.04$ mm^3. Two gold wires of 15 μm in diameter were attached to the sample using gold or carbon paste for electrical measurement. The electrode gap was about 0.3×0.5 mm^2.

The pulsed voltage applied along the *a*-axis was relatively high up to 20 V (670 V/cm). The *I*–*V* relationship, however, remained linear in this range without light. Under an electric field of 500 V/cm, the current in the sample was only about 20 nA at 4 K.

In this experiment, a pulsed laser with polarizations along the *a*- and *b*-axes and with a wave vector (*k*) perpendicular to the two-dimensional (*ab*) plane was used for the excitation. The photon energy was 2.6 eV (450 nm) and the pulse duration was about 5 ns. The application timing of the laser pulse and the voltage pulse is depicted in Fig. 2(a). The photocurrent was monitored with a digitizing oscilloscope. In order to investigate the fast response, we measured the photocurrent across a 50 Ω reference resistor.

Figure 2(b) shows the time evolution of the photocurrents for the $E \parallel a$- and $E \parallel b$-polarizations under an electric field of 470 V/cm at 4 K. There exists a qualitative difference in induced photocurrent between these two polarization conditions. When the light polarized along the *a*-axis was applied, a photocurrent with a decay time of about 5 ns was observed. Strength increased linearly with excitation intensity and electric field.

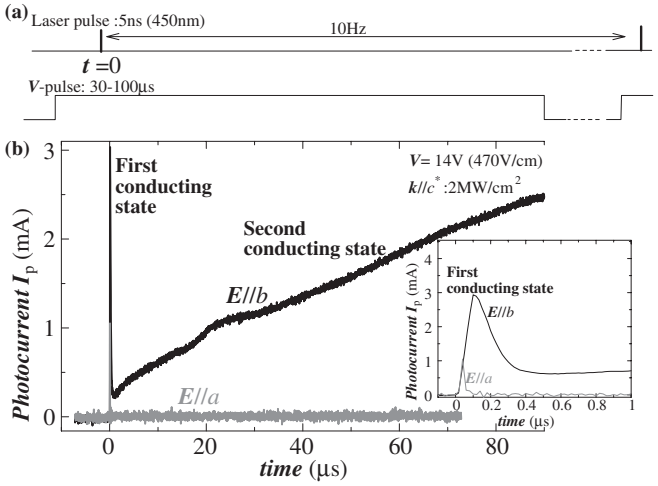

Fig. 2. (a) Application timing of laser pulse with photon energy of 2.6 eV (450 nm) and electric field pulse. (b) Time evolution of photocurrent for α-(BEDT-TTF)$_2$I$_3$ at 4 K. The photocurrent can be separated in two types by the polarized light along the *a*- (gray line, $E \parallel a$) and *b*- (black line, $E \parallel b$) axes, respectively. The laser power is 2 MW/cm^2 and the electric field is 470 V/cm. The earlier time region up to 1 μs is expanded in the inset.

A significant feature in Fig. 2(b) is the large photocurrent with two components observed for the $E \parallel b$-polarization. The first component had a life time of about 120 ns. After about 0.7 μs, the second component started to grow and remained persistently, that is, it could be kept as long as the electric field was applied. Notably, the resistivity was less than 0.36 Ω·cm for the first component and was reduced by about seven orders of magnitude from that (∼4 MΩ·cm) in the CO state without the light. This estimation is based on the laser spot size in the electrode gap and the penetration depth of the light (assumed to be 1 μm). For the second component after 80 μs, the resistivity was also reduced to less than 0.4 Ω·cm. These values are comparable to that in the metallic state of this material under a high pressure.[4] Thus, the anomalous photocurrent for the $E \parallel b$-polarization suggests that two photo-induced metallic states appeared successively. Hereafter, we call them the first conducting state and the second conducting state. In this study, we focus our attention on the anomalous photocurrent for the $E \parallel b$-polarization.

A possibility that the anomalous photocurrent is due to the thermal effect can be ruled out by the following reasons. (1) The anomalous photocurrent decreased with increasing temperature and disappeared above 50 K. (2) As discussed below, the effective mobility in the first conducting state under the electric field of 270 V/cm and the excitation intensity of 2 MW/cm^2 is more than 1000 cm^2/(V·s) at 4 K. On the other hand, the carrier mobility in the metallic state above 135 K under ambient pressure is less than 10 cm^2/(V·s). This means that the first conducting state is different from the pristine metallic state above 135 K. (3) The second component shows prominent thresholds in the electric field and laser power dependences, as described below. (4) The maximum laser power per one pulse was about 80 μJ in this experiment. Considering the specific heat $C_p \sim 5$ mJ/(g·K) at 4 K, the temperature of the sample should be lower than 40 K, even if all the laser power was used for the sample heating. In addition, the temperature change induced by self-generation of heat (35 mW at 80 μs) due to the high voltage (14 V) should be less than 10 deg. (5) Recently, we have found that β'-(BEDT-TTF)$_2$ICl$_2$ which is an insulator ($\rho = 100$ Ω·cm at room temperature) throughout temperature region also exhibits the photo-induced I–M transition under the same experimental condition.[20]

Let us consider the dependences of the anomalous photocurrent for the $E \parallel b$-polarization in Fig. 2(b) on the laser power (Fig. 3), the applied electric field (Figs. 4 and 5), and the onset of the pulsed voltage (Fig. 6). The laser power dependence of the photocurrent under the electric field of 470 V/cm at 4 K is shown in Fig. 3. The maximum laser power is 2 MW/cm^2 at 100%. The inset is the laser power dependence on the intensity of the two components after 5 ns and 30 μs. Figures 4 and 5, on the other hand, show the time evolution of the photocurrent under the several electric fields for the laser power of 2 MW/cm^2. The electric field dependence of the intensity of the two components (after 5 ns and 80 μs) is shown in the inset of Fig. 4. Lastly, we show the effect of timing of the applied voltage pulse on the two components in Fig. 6.

First, we discuss the first conducting state. The first conducting state was sensitive to the applied excitation

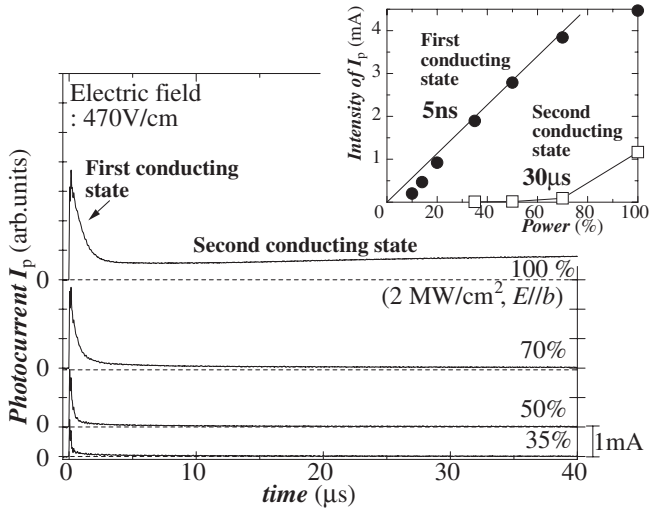

Fig. 3. Time evolution of photocurrent for $E \parallel b$-polarization under several laser power conditions up to 2 MW/cm^2 (100%) under electric field of 470 V/cm. The inset shows the laser power dependency of the photocurrent intensity in the first conducting (after 5 ns: ●) and second conducting (after 30 μs: □) states.

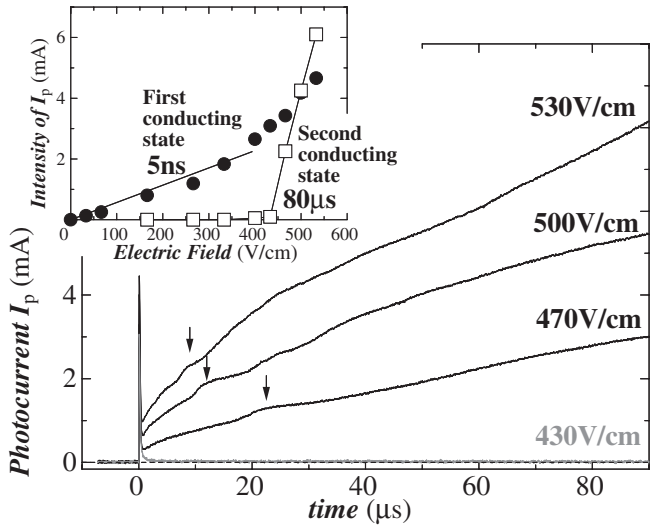

Fig. 4. Time evolution of photocurrent for the $E \parallel b$-polarization under several electric field conditions up to 530 V/cm and the laser power of 2 MW/cm^2. The inset is the applied voltage dependent of the photocurrent intensities in the first conducting (after 5 ns: ●) and the second conducting (after 80 μs: □) states. As for the small hump indicated by the arrow, see text.

intensity and exhibited an almost linear response up to 1.4 MW/cm^2 (70%) as shown in the inset of Fig. 3. The strength of the photocurrent exhibited also a linear response to the applied electric field of up to about 330 V/cm (inset of Fig. 4) and this state is independent of the timing of the applied voltage pulse as shown in Fig. 6. In this first conducting state, almost constant current was observed during the initial (about) 100 ns under the electric field above 270 V/cm (Fig. 5). This is because the carriers have high drift velocity and can travel between the electrodes within their lifetime (about 120 ns). Under the low electric field below 170 V/cm, on the other hand, it decreased gradually even in this time region. This indicates that the drift velocity

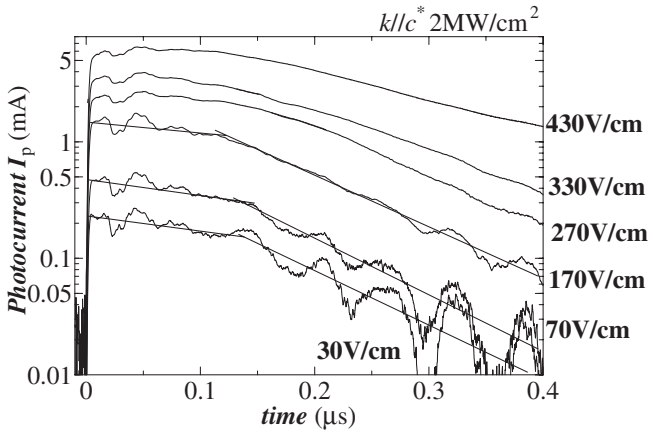

Fig. 5. Photocurrent for $E \parallel b$-polarization in the first conducting state under the electric field below 430 V/cm. It should be noted that the slow and rapid oscillations are artifacts due to the ringing of the applied voltage pulse.

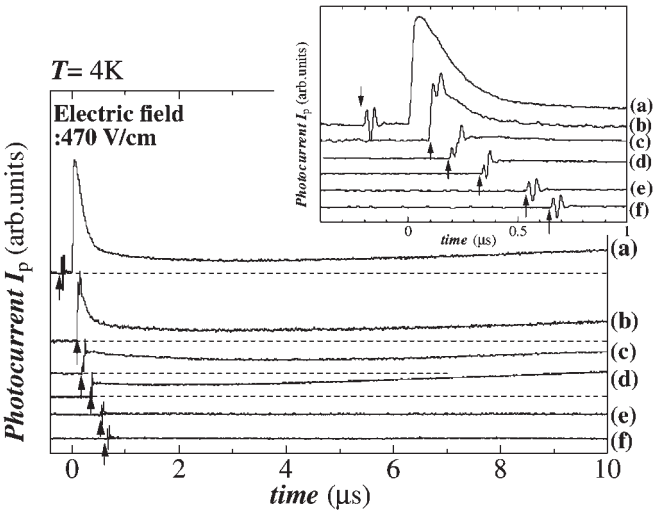

Fig. 6. Photocurrent for $E \parallel b$-polarization depending on timing of electric field pulse of 470 V/cm at 4 K. Each arrow represents an onset of the electric field pulse. The earlier time region up to 1 μs is shown expanded in the inset.

of the carriers is low and then the carriers cannot travel between electrodes within their lifetime. Based on these results, we can roughly estimate the drift mobility as 1000 cm^2/(V·s).

We have attempted another estimation of the effective mobility. The intensity of the photocurrent was sensitive to the magnetic field (H) perpendicular to the ab plane. The magnetoresistance ($\Delta\rho_H/\rho_0$) increased as a linear function of H^2 up to the magnetic field of 3 T ($\Delta\rho_H/\rho_0 \sim 0.15$) at 4 K.[21] According to the relation $\Delta\rho_H/\rho_0 = \mu^2 H^2$, the effective mobility (magnetoresistance mobility) μ is estimated to be about 1300 cm^2/(V·s) from the slope. This value is comparable to those of typical quasi two-dimensional organic metals such as θ-(BEDT-TTF)$_2$I$_3$, which suggests probable observation of the quantum effect at the high magnetic field above 10 T. The investigation under the high magnetic field will give important information on the first conducting state.

The revival of the conduction and the persistently

conducting behavior associated with the second conducting state were observed as long as a high electric field was applied under the high laser power. Under a low laser power or low electric field, the photocurrent decayed rapidly toward zero and the system returned to the CO state (Figs. 3 and 4). Figure 3 indicates that the second conducting state was observed at a laser power above 1.4 MW/cm^2 (70%), when the applied electric field was fixed at 470 V/cm. On the other hand, when the applied laser power was fixed at 2 MW/cm^2, this state appeared clearly under the electric field above 470 V/cm (Fig. 4). Under the electric field above 500 V/cm, the conductivity in the second conducting state became higher than that in the first conducting state. In this sense, the second conducting state is a metal (highly conducting) state that is different from the first conducting state. The intensity of the photocurrent in the second conducting state exhibited highly nonlinear responses to both of the applied laser power and the electric field, each of which was accompanied by a threshold behavior as shown in the insets of Fig. 3 (□: 30 μs) and Fig. 4 (□: 80 μs). Under the conditions where the second conducting state appears, the voltage dependence of the photocurrent in the first conducting state shows a deviation from a linear line (above about 430 V/cm in the inset of Fig. 4; ●).

The second conducting state was investigated by changing the timing of the applied voltage pulse (14 V, 470 V/cm) under the excitation intensity of 2 MW/cm^2 at 4 K (Fig. 6). Each arrow in Fig. 6 indicates an onset of the pulsed voltage. The second conducting state appeared in the runs (a)–(d). In the runs (e) and (f), on the contrary, the second conducting state was absent, and even the application of a higher voltage up to 20 V (670 V/cm) could not induce the second conducting state. Figure 6 strongly suggests that the high electric field cannot induce the second conducting state once the system returns to the CO state. The first conducting state and the high electric field or high current density should be correlated to the growth process of the second conducting state. It is plausible that the high electric field applied before the system returns to the CO state disturbs the charge-ordering pattern and then brings about the nonlinear conductivity. The electric field dependence of the small hump in the photocurrent curve in Fig. 4 implies the dynamics of this process.

Lastly, our results should be compared with those of the perovskite manganite $Pr_{0.7}Ca_{0.3}MnO_3$ reported by Miyano *et al.*[16] In our system, the second conducting state was observed under the excitation intensity at least 10 times lower than that for $Pr_{0.7}Ca_{0.3}MnO_3$. In addition, the qualitative difference lies in the electric field dependence of the first component of the photocurrent. In $Pr_{0.7}Ca_{0.3}MnO_3$, the intensity of the photocurrent is a highly nonlinear function of the applied voltage. In the present system, on the other hand, the photocurrent in the first conducting state exhibited a linear response to the applied voltage as shown in the inset of Fig. 4.

In conclusion, we have revealed the time evolution of the photocurrent in the CO state of the organic conductor α-(BEDT-TTF)$_2$I$_3$ at 4 K. The photocurrent can be separated in two types by the polarized light along the *a*- and *b*-axes. Two conducting states (the first and second conducting states) were induced by the $E \parallel b$-polarization. The resistivity decreased by about seven orders in each state. The first conducting state disappeared within about 120 ns. The carriers in this state have a high effective mobility of more than 1000 cm^2/(V·s). On the other hand, the second conducting state appeared as long as the high electric field was applied, and was accompanied by the prominent threshold behaviors for both laser power and electric field.

The interrelations among the charge-ordered state, the photo-induced metallic state, and the persistently conducting state remain to be determined. Further investigation, however, will lead us to interesting photo-induced phenomena derived from the charge-ordered state associated with the strong correlation.

Acknowledgmet

This work was partially supported by Grants-in-Aid for Scientific Research (Nos. 14740223, 15750129 and 16GS50219) from the Ministry of Education, Culture, Sports, Science and Technology of Japan.

1) H. Taniguchi, M. Miyashita, K. Uchiyama, K. Satoh, N. Mori, H. Okamoto, K. Miyagawa, K. Kanoda, M. Hedo and Y. Uwatoko: J. Phys. Soc. Jpn. **72** (2003) 468.
2) M. Maesato, Y. Kaga, R. Kondo and S. Kagoshima: Rev. Sci. Instrum. **71** (2000) 176.
3) N. Tajima, M. Tamura, Y. Nishio, K. Kajita and Y. Iye: J. Phys. Soc. Jpn. **69** (2000)543.
4) N. Tajima, A. Ebina-Tajima, M. Tamura, Y. Nishio and K. Kajita: J. Phys. Soc. Jpn. **71** (2002) 1832.
5) S. Tomić, J. R. Cooper, D. Jérome and K. Bechgaard: Phys. Rev. Lett. **62** (1989) 462.
6) N. Toyota, Y. Abe, T. Kuwabara, E. Negishi and H. Matsui: J. Phys. Soc. Jpn. **72** (2003) 2714.
7) S. Uji, H. Shinagawa, T. Terashima, T. Yakabe, Y. Terai, M. Tokumoto, A. Kobayashi, H. Tanaka and H. Kobayashi: Nature **410** (2001) 908.
8) T. Takahashi, D. Jérome and K. Bechgaard: J. Phys. Lett. (Paris) **51** (1982) L565.
9) D. Andres, M. V. Kartsovnik, P. D. Grigoriev and H. Müller: Phys. Rev. B **68** (2003) 201101(R).
10) K. Bender, I. Hennig, D. Schweitzer, K. Dietz, H. Endres and H. J. Keller: Mol. Cryst. Liq. Cryst. **108** (1984) 359.
11) R. P. Shibaeva, V. F. Kaminskii and E. B. Yagubskii: Mol. Cryst. Liq. Cryst. **119** (1985) 361.
12) H. Kobayashi, R. Kato, A. Kobayashi, Y. Nishio, K. Kajita and W. Sasaki: Chem. Lett. (1986) 833.
13) H. Kobayashi, R. Kato, A. Kobayashi, Y. Nishio, K. Kajita and W. Sasaki: Chem. Lett. (1986) 789.
14) H. Kino and H. Fukuyama: J. Phys. Soc. Jpn. **64** (1995) 1877.
15) Y. Takano, K. Hiraki, H. M. Yamamoto, T. Nakamura and T. Takahashi: J. Phys. Chem. Solids **62** (2001) 393.
16) K. Miyano, T. Tanaka, Y. Tomioka and Y. Tokura: Phys. Rev. Lett. **78** (1997) 4257.
17) M. Fiebig, K. Miyano, Y. Tomioka and Y. Tokura: Appl. Phys. B **71** (2000) 211.
18) F. O. Karutz, J. U. von Schütz, H. Wachtel and H. C. Wolf: Phys. Rev. Lett. **81** (1998) 140.
19) N. Uchida, S. Koshihara, T. Ishikawa, A. Ota, S. Fukaya, M. Chollet, H. Yamochi and G. Saito: J. Phys. IV (Paris) **114** (2004) 143.
20) N. Tajima, J. Fujisawa, R. Kato, T. Ishihara, H. Taniguchi, Y. Nishio and K. Kajita: in preparation.
21) Details of the magnetic field effects on the photoconductivity will be described in the next paper.